

ELECTROCONVECTION NEAR TWO-LAYER COMPOSITE MICROPARTICLES

© 2025 G. S. Ganchenko^a, V. S. Shelistov^{a, *}, and E. A. Demekhin^{a, b}

^a*Laboratory of Micro- and Nanoscale Electro- and Hydrodynamics,
Financial University under the Government of the Russian Federation, Moscow, Russia*

^b*Laboratory of General Aerodynamics, Institute of Mechanics,
Lomonosov Moscow State University, Moscow, Russia*

*e-mail: shelistov_v@mail.ru

Received August 06, 2024

Revised September 16, 2024

Accepted September 18, 2024

Abstract. This paper presents the results of a numerical simulation of an electrolyte solution behavior near a spherical dielectric microparticle covered with a homogeneous ion-selective shell under the influence of an external electric field. The particle is assumed to be stationary, and the electrolyte either stays still or is pumped externally with a constant velocity in absence of the electric field. The field, in turn, generates electroosmotic flow near the particle's surface. It is shown that concentration polarization can occur near the particle, whereas electrokinetic instability only occurs near particles with a sufficiently thick shell. When the particle's surface charge is opposite to the one of its shell, non-stationary regimes may be observed when the shell is thin enough.

Keywords: *electrophoresis, electroosmosis, composite particle, concentration polarization, instability, numerical simulation*

DOI: 10.31857/S00232912250102e9

INTRODUCTION

The study of electroosmosis near solid particles is inextricably linked to the study of electrophoresis [1]. The forces generated by electroosmotic motion act on the particle immersed in the electrolyte. By the beginning of the 21st century, the study of the motion of microparticles and fluids in microscales – microfluidics – has gained special interest. In particular, electrophoresis finds application in labs-on-chip for solving problems of medical diagnostics and chemical analysis [2].

One of the main characteristics of electrophoresis is the dependence of the velocity developed by a microparticle on the properties of the electric field: this dependence turns out to be different for different types of particles. Smoluchowski [1] studied the motion of dielectric particles and established the linear character of the dependence of their velocity on the field strength. Later Dukhin showed [3] that the considered dependence is more complicated, and in theoretical works of Yariv's group [4–6] a deviation from the linear dependence was predicted for strong fields and strongly charged particles. Experimental confirmation of this prediction was obtained by Tottori [7]. A review of modern concepts of dielectric particle electrophoresis can be found in Khair [8].

Electrophoresis of ion-selective particles in liquid electrolyte shows a much more complex behavior due to the presence of concentration polarization and electrokinetic processes of the second kind [9–14]. The electrophoresis rate maintains the linear dependence on the field strength as long as it is small [11], but as the strength increases, the dependence becomes more complicated [12], and in strong fields unsteady flow regimes with various types of instabilities arise [13, 14].

When studying the behavior of more complex particles, like biological ones, the assumption of particle homogeneity turns out to be inapplicable [15, 16]. One of the simplest ways to overcome this obstacle is to consider composite particles with a fixed internal structure. The model of “soft” particles [17, 18], having a homogeneous core impermeable to the electrolyte and a homogeneous shell permeable to salt ions, has been quite successful. At the same time, there is a noticeable lack of theoretical research in this direction, and the existing works usually use significant simplifications (in particular, linearization of motion equations). A semi-analytical approach based on the splicing of asymptotic expansions, actively used by Yariv's group for both electrophoresis [6] and related electrokinetics problems [19], should be separately

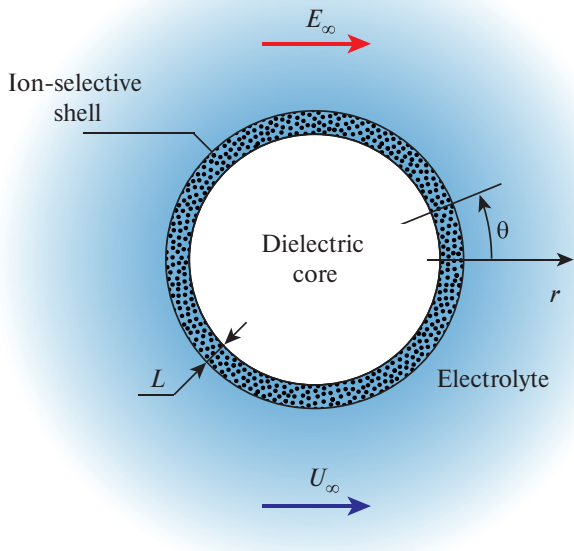


Fig. 1. Schematic representation of a composite micro-particle.

emphasized. Nevertheless, the possibilities of analytical study of electrokinetics are approaching the limit, and further development requires the use of direct numerical simulation.

In the present work, we attempt to fill this gap and model the motion of a “soft” particle in a nonlinear statement with minimal simplifications. The results of numerical modeling can be used to predict the modes of motion arising in experiments and create a foundation for the development of labs-on-chip for manipulating complex biological particles.

PROBLEM STATEMENT AND SOLUTION METHODOLOGY

We consider a spherical microparticle consisting of a spherical electroneutral dielectric core of radius \tilde{r}_0 and a homogeneous uniformly charged shell made of an ion-selective layer of thickness \tilde{L} (Fig. 1). The core’s surface is assumed to carry a uniform surface charge density $\tilde{\sigma}$, and the volumetric charge density of the shell is \tilde{N} . The particle is stationary and is bathed by a solution of electroneutral symmetric binary electrolyte with ion concentrations \tilde{C}_∞ , which is pumped at an external velocity \tilde{U}_∞ . To simplify the mathematical formulation, the value of \tilde{C}_∞ is assumed to be sufficiently small, the charge numbers of the salt ions are assumed to be ± 1 , and their diffusion coefficients are assumed to be equal. These simplifications are valid, for example, for KCl solutions with concentration up to hundreds of mol/m^3 , and allow us reducing the number of parameters of the problem. An external electric field of strength \tilde{E}_∞ acts on the system. This formulation is

similar to the one for electrophoresis [20], but \tilde{U}_∞ acts as an additional parameter.

If we neglect chemical reactions and dissociation of the solvent liquid, the behavior of dilute electrolyte ions can be described by the system of Nernst–Planck equations, which should be complemented by the Poisson equation describing the electric potential distribution and the Navier–Stokes equations for the velocity field. Due to the smallness of characteristic Reynolds numbers, the Navier–Stokes equations are taken in the Stokes approximation:

$$\frac{\partial \tilde{C}^\pm}{\partial \tilde{t}} + \tilde{\mathbf{U}} \cdot \tilde{\nabla} \tilde{C}^\pm = \pm \frac{\tilde{D} \tilde{F}}{\tilde{R} \tilde{T}} \tilde{\nabla} \cdot (\tilde{C}^\pm \tilde{\nabla} \tilde{\Phi}) + \tilde{D} \tilde{\nabla}^2 \tilde{C}^\pm; \quad (1)$$

$$\tilde{\varepsilon} \tilde{\nabla}^2 \tilde{\Phi} = -\tilde{F} (\tilde{C}^+ - \tilde{C}^-); \quad (2)$$

$$\tilde{\nabla} \tilde{\Pi} - \tilde{\mu} \tilde{\nabla}^2 \tilde{\mathbf{U}} = -\tilde{F} (\tilde{C}^+ - \tilde{C}^-) \tilde{\nabla} \tilde{\Phi}; \quad (3)$$

$$\tilde{\nabla} \cdot \tilde{\mathbf{U}} = 0. \quad (4)$$

It is convenient to solve equations (1)–(4) in a spherical coordinate system with the origin at the center of the particle. Since the system has axial symmetry along the electric field direction, it is solved in axisymmetric formulation, so the spatial variables are the radius \tilde{r} and azimuthal angle $0 \leq \theta \leq \pi$. The unknowns are the molar ion concentrations \tilde{C}^\pm , the electric potential $\tilde{\Phi}$, the pressure $\tilde{\Pi}$ and the velocity vector $\tilde{\mathbf{U}}$. The symbol \tilde{F} denotes the Faraday constant, \tilde{R} is the universal gas constant, and \tilde{T} is the absolute temperature, which is assumed to be constant. The diffusion coefficient of electrolyte ions is denoted by \tilde{D} , the dynamic viscosity of the electrolyte is denoted by $\tilde{\mu}$, its absolute dielectric constant is denoted by $\tilde{\varepsilon}$. The last two quantities are assumed to be constant, independent of the local ion concentration. The dielectric constant of the core is denoted by $\tilde{\varepsilon}_p$, and the dielectric constant of the shell, which is filled with electrolyte, is assumed to be $\tilde{\varepsilon}$. The ion diffusion coefficients in the shell are for simplicity assumed to be \tilde{D} as well. The tilde in notations denotes dimensional quantities.

The following characteristic quantities have been chosen for making the system dimensionless: core radius \tilde{r}_0 , diffusion coefficient \tilde{D} (included in the characteristic time \tilde{r}_0^2/\tilde{D} and characteristic velocity \tilde{D}/\tilde{r}_0), thermal potential $\tilde{\Phi}_0 = \tilde{R}\tilde{T}/\tilde{F}$, concentration \tilde{C}_∞ , and viscosity $\tilde{\mu}$. Note that the choice of the diffusion velocity as the characteristic velocity simultaneously allows taking zero pumping velocity and does not introduce constraints into the hydrodynamics. Two dimensionless parameters appear in dimensionless equations (1)–(4): the Debye number $\nu = \tilde{\lambda}_D^2/\tilde{r}_0$, where $\tilde{\lambda}_D^2 = \tilde{\varepsilon}\tilde{R}\tilde{T}/\tilde{F}^2\tilde{C}_\infty$ is the square of the electric double layer thickness, and the coupling coefficient between the hydrodynamic and electrostatic parts of the problem $\kappa = \tilde{\varepsilon}\tilde{\Phi}_0^2/\tilde{\mu}\tilde{D}$. The equations eventually take the form

$$\frac{\partial C^\pm}{\partial t} + \mathbf{U} \cdot \nabla C^\pm = \pm \nabla \cdot (C^\pm \nabla \Phi) + \nabla^2 C^\pm; \quad (5)$$

$$\nu^2 \nabla^2 \Phi = C^- - C^+; \quad (6)$$

$$-\nabla \Pi + \nabla^2 \mathbf{U} = \frac{\kappa}{\nu^2} (C^+ - C^-) \nabla \Phi; \quad (7)$$

$$\nabla \cdot \mathbf{U} = 0. \quad (8)$$

Equations (5)–(8) in this form are not applicable in all spatial areas. For example, no electrolyte penetrates into the core, so at $r < 1$ $C^\pm = \mathbf{U} = 0$ and only equation (6) reduced to the Laplace equation remains of the whole system. For convenience in setting the boundary conditions, we denote the electric potential inside the core by ϕ :

$$\nabla^2 \phi = 0. \quad (9)$$

Inside the shell, $1 < r < 1 + L$, there is no electrolyte motion, $\mathbf{U} = 0$, and equations (5)–(6) take the form

$$\frac{\partial C^\pm}{\partial t} = \pm \nabla \cdot (C^\pm \nabla \Phi) + \nabla^2 C^\pm; \quad (10)$$

$$\nu^2 \nabla^2 \Phi = C^- - C^+ - N, \quad (11)$$

where $N = \tilde{N}/\tilde{C}_\infty$ is dimensionless volumetric charge density. This parameter determines the ability of the shell to attract ions of the same sign and repel ions of the opposite sign: at $N = -\infty$ the shell is perfectly cation-selective, at $N = +\infty$ – perfectly anion-selective. More details about its influence are given in [21] on the example of a flat membrane.

The considered formulation contains several boundaries, on each of which different conditions are imposed. All

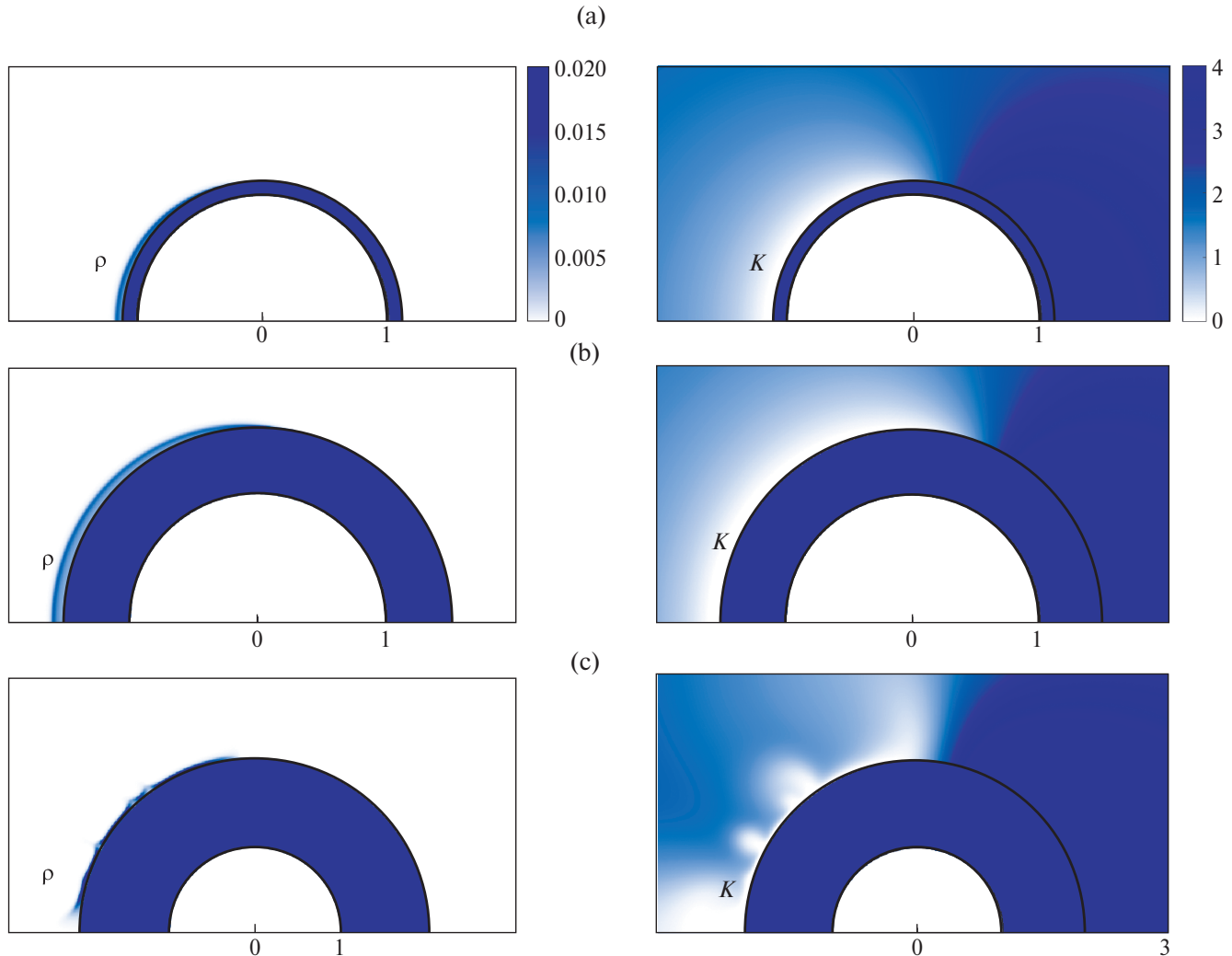


Fig. 2. Distributions of charge density $\rho = C^+ - C^-$ and salt concentration $K = C^+ + C^-$ outside the particle at $E_\infty = 10$, $U_\infty = 0$ and $\sigma = 0$. (a) $L = 0.1$, (b) $L = 0.5$, (c) $L = 1.0$. The distributions inside the shell are not shown.

unknown functions are assumed to be continuous in the whole domain. At the boundaries $\theta = 0$ and $\theta = \pi$, symmetry conditions are set for C^\pm , Φ and normal velocity components U_r , and antisymmetry condition for the tangential component $U_\theta = 0$. At $r = 0$, the zero level of potential, $\phi = 0$, is assumed and the condition of absence of singularity is imposed. At the boundary of the core, $r = 1$, one should expect a jump of the field strength by the value $\delta = \tilde{\epsilon}_p/\tilde{\epsilon}$ and the absence of ion flux:

$$\begin{aligned} r = 1: \Phi = \phi; v \frac{\partial \Phi}{\partial r} = \delta v \frac{\partial \phi}{\partial r} - \sigma; \\ \pm C^\pm \frac{\partial \Phi}{\partial r} + \frac{\partial C^\pm}{\partial r} = 0. \end{aligned} \quad (12)$$

On the boundary of the shell, $r = 1 + L$, simple no-slip and no-flux conditions, $U = 0$, which ensure the continuity of the velocity field, are assumed. They can be considered as a special case of liquid slip conditions near a hydrophobic surface [22]. At a distance from the particle, the ion concentrations tend to the equilibrium value, the field strength tends to the one of the external field, and the velocity tends to the one of the incoming flow:

$$\begin{aligned} r \rightarrow \infty: C^\pm \rightarrow 1; \Phi \rightarrow -E_\infty r \cos \theta; \\ U_r \rightarrow U_\infty \cos \theta; U_\theta \rightarrow U_\infty \sin \theta. \end{aligned} \quad (13)$$

Finally, the electrolyte is assumed to be undisturbed at the initial time instant:

$$t = 0; C^\pm = 1. \quad (14)$$

This condition does not take into account the redistribution of ions due to the charge present in the particle, but calculations show that such redistribution occurs very quickly (within a few time steps) and does not affect the further behavior of the system.

To solve the system (5)–(14), we use a modification of the finite-difference method of the second-order approximation in space and the third-order approximation in time, previously used to solve the electrophoresis problem [20]. At each time step, the stationary equations (6)–(9) are transformed into systems of ordinary differential equations using the eigenfunction expansion of the differential operators with respect to the angle. The system for (9) is solved analytically and substituted into boundary conditions (12), the other equations are written in difference form and reduced to systems of linear algebraic equations with 3- and 5-diagonal matrices, which are solved by the tridiagonal matrix algorithm and its extension to 5-diagonal matrices. The found potential and velocity distributions are substituted into equations (5), which are integrated by the semi-implicit Runge–Kutta method [23].

In the calculations presented below, the following parameter values have been fixed: $v = 10^{-3}$, $\kappa = 0.2$,

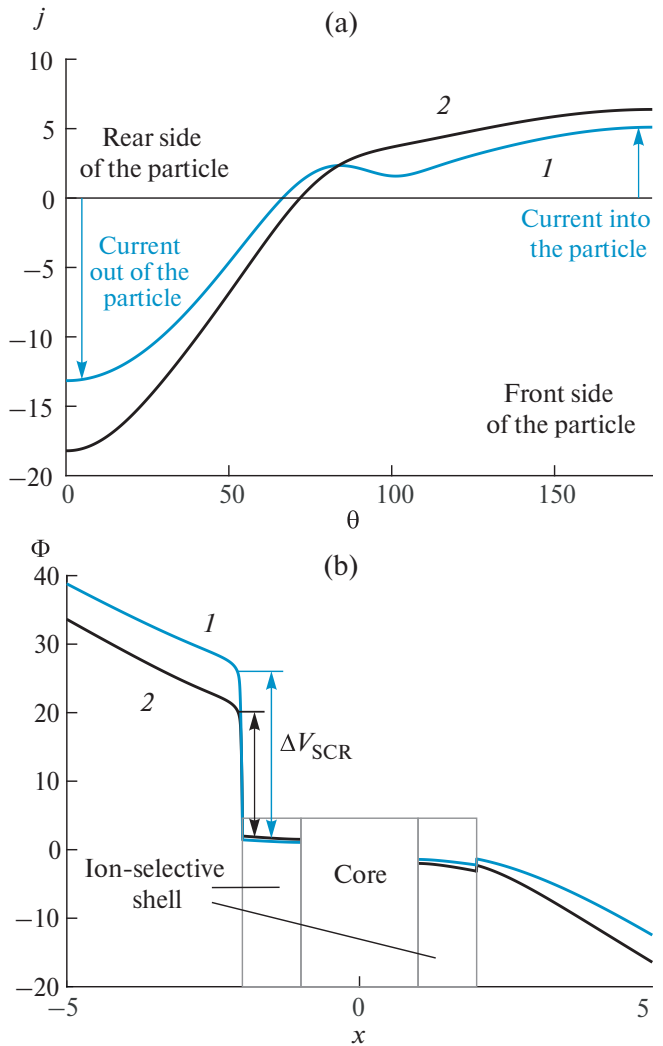


Fig. 3. Distributions of (a) current through the surface $j^+(\theta)$ and (b) electric potential Φ along the symmetry axis $x = r \cos \theta$ at $E_\infty = 5$, $\sigma = 0$ and $L = 1.0$. Curves 1— $U_\infty = 0$, curves 2— $U_\infty = 50$.

$N = -10$ (cation-selective shell with good selectivity), $\delta = 0.05$. The external electric field strength E_∞ , the surface charge density of the core σ and the velocity of the incoming electrolyte U_∞ were varied, remaining constant within each of the calculations, with the direction of E_∞ and U_∞ following the scheme in Fig. 1.

RESULTS AND DISCUSSION

When comparing electrophoresis of dielectric and ion-selective particles, the main difference is the presence of electric current through the particle surface. For the problem under consideration, it also seems logical to estimate the current through the shell boundary:

$$j^+(\theta) = \left(C^+ \frac{\partial \Phi}{\partial r} + \frac{\partial C^+}{\partial r} \right) \Big|_{r=1+L}.$$

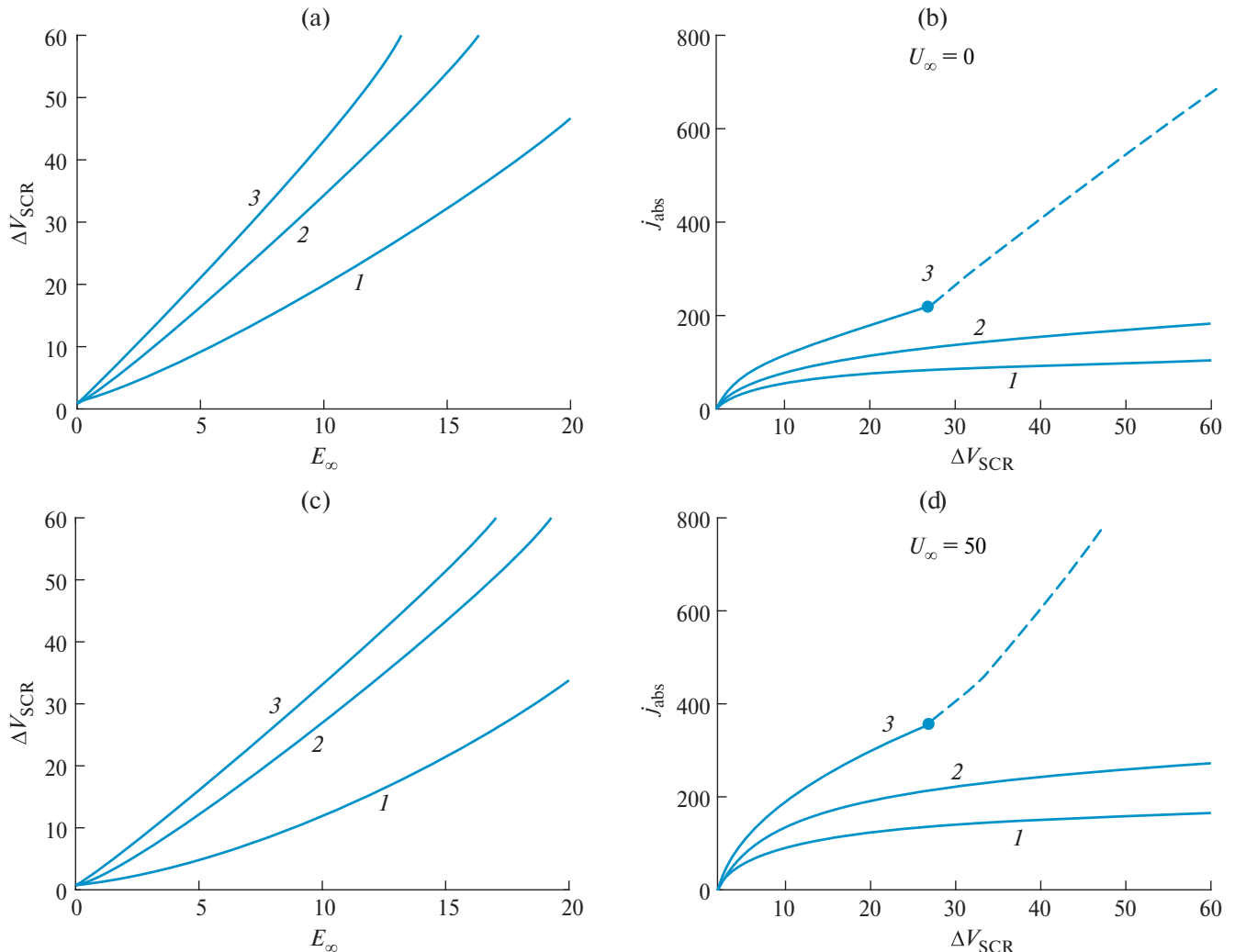


Fig. 4. (a), (c) – dependence of voltage drop in the space charge region ΔV_{SCR} on the external field strength E_∞ ; (b), (d) – dependence of integral current j_{abs} on ΔV_{SCR} . Graphs (a) and (b) are plotted without advection, $U_\infty = 0$, graphs (c) and (d) – with advection, $U_\infty = 50$. Curves 1 are $L = 0.1$, curves 2 are $L = 0.5$, curves 3 are $L = 1.0$. In all cases $\sigma = 0$. The dotted line corresponds to non-stationary modes (with electroconvection), for which the current values are averaged over time.

According to the scheme in Fig. 1, cations enter the shell from the left, $\theta > \pi/2$, and exit from the right, $\theta < \pi/2$. In stationary modes, the total charge of the shell remains

unchanged, so the condition $\int_0^\pi j^+(\theta) \sin \theta d\theta = 0$ is satisfied. In the general case this condition can be violated (in particular, at $t = 0$).

Ion-selective surfaces are characterized by concentration polarization – redistribution of electrolyte ions near such a surface due to the influence of an external field with desalination and formation of a space charge area on the anode side, as well as with salt accumulation on the cathode side [11]. In sufficiently strong fields, the salt concentration can significantly exceed the equilibrium one [13]. Fig. 2 shows the charge and total ion concentration distributions in a still electrolyte near

particles with different shell thicknesses. As it can be seen, concentration polarization takes place even near a thin shell.

Fig. 3 shows characteristic distributions of the current through the shell boundary and the electric potential along the symmetry axis. In the graph (b) one can note a significant voltage drop in the space charge region, denoted by ΔV_{SCR} , which in combination with the current through the particle generates electrokinetic instability. The electroconvection caused by the instability is clearly visible in plot (c) in Fig. 2c.

While the velocity value U_∞ is usually used to estimate the electrophoresis intensity, it is convenient to estimate the electroosmosis intensity near a stationary particle by the integral current. In the present work, the value

$$j_{\text{abs}} = 2\pi \left(1 + L^2\right) \int_0^{\pi} |j(\theta) \sin \theta| d\theta$$

is introduced for this purpose.

By plotting the values ΔV_{SCR} and j_{abs} , realized in different modes, it is possible to construct the current-voltage characteristics of the microparticle. Examples of such characteristics are shown in Fig. 4. The dependence of ΔV_{SCR} on E_{∞} , as shown in graphs (a) and (c), is almost linear. Graphs (b) and (d) demonstrate behavior similar to electromembrane systems: at low voltage drops, the underlimiting regime is realized (proportionally in proportion to voltage), at moderate voltage drops, the limiting mode is realized (current growth slows down sharply). When the shell thickness is large enough, even the overlimiting regime is realized: when the critical value of ΔV_{SCR}^* is exceeded, electroconvection occurs, intensifying the current. The observed value ΔV_{SCR} corresponds to the theoretical predictions of [24].

In Fig. 4, there is a noticeable increase in the current through the particle with increasing thickness of its shell. This is largely due to the increase in the surface area of the particle. At the same time, with increasing shell thickness, the voltage drop in the space charge region also increases, so a stronger field is required for electroconvection to occur near particles with thin shells. Advection does not qualitatively affect the behavior of the system: the voltage drop slightly decreases, the current increases. The current increase is due to the convective inflow of charge carriers into the desalination zone. The flow structure did not undergo qualitative changes even at $U_{\infty} = 1,000$. The slip of the liquid near the shell was not considered in the present work, but its contribution can be expected to be quantitative as well, expressing itself mainly in the shift of the threshold of instability onset to the left [25].

The influence of the charge of the core surface on the effects described above was so insignificant that it is not shown in the diagrams. Any significant effect is observed only in the case when the shell thickness is small and its charge is opposite in sign to the charge of the core surface. This case is studied by the authors in a separate paper, the preprint of which is available on request [26].

Finally, we note that when the absolute value of the shell charge decreases, its selectivity decreases and conductivity increases, which leads to a decrease in ΔV_{SCR} . As a consequence, a stronger field must be applied for a noticeable concentration polarization to occur, and the critical value of ΔV_{SCR}^* shifts to the right. Nevertheless, the shell thickness even in this case determines whether electroconvection will occur at all. Here it is necessary to emphasize the difference of the considered formulation from the electromembrane system with a non-ideal membrane [21]: if in the latter the membrane conductivity plays a determining role in the conductivity of the whole system, in the considered formulation the ion flux can bypass the particle, so the conductivity of the system is determined by the conductivity of the electrolyte.

CONCLUSION

The paper presents the results of numerical simulation of electrokinetics in electrolyte near a spherical dielectric microparticle covered with an ion-selective shell. It is shown that concentration polarization occurs near the shell, regardless of its thickness, but electroconvection can occur only at a sufficiently large thickness of the shell. The electrolyte pumping and the charge on the dielectric surface have no qualitative effect on the dynamics of the system. The results of this work can be used to develop methods for controlling composite microparticles, including biological ones, and to develop methods for investigating the structure of such particles in microdevices.

FUNDING

The work was financially supported by RSF (grant 22-79-10085).

ETHICS DECLARATION

There are no human or animal studies in this paper.

CONFLICT OF INTERESTS

The authors of this paper declare that they have no conflict of interests.

REFERENCES

1. *Paillet R. M. Smoluchowski — Contribution à la théorie de l'endosmose électrique et de quelques phénomènes corrélatifs* (Bulletin de l'Académie des Sciences de Cracovie, mars 1903) // *J. Phys.: Theor. Appl.* 1904. Vol. 3. No. 1. P. 912. <https://doi.org/10.1051/jphystap:019040030091201>
2. *Mohammadi R., Afsaneh H., Rezaei B., Zand M.M.* On-chip dielectrophoretic device for cancer cell manipulation: A numerical and artificial neural network study // *Biomicrofluidics*. 2023. Vol. 17. P. 024102. <https://doi.org/10.1063/5.0131806>
3. *Dukhin S.S., Deryagin B.V.* *Electrophoresis*. M.: Nauka. 1976.
4. *Schnitzer O., Yariv E.* Strong-field electrophoresis // *J. Fluid Mech.* 2012. Vol. 701. Pp. 333–351. <https://doi.org/10.1017/jfm.2012.161>
5. *Schnitzer O., Zeyde R., Yavneh I., Yariv E.* Weakly nonlinear electrophoresis of a highly charged colloidal particle // *Phys. Fluids*. 2013. Vol. 25. No. 5. P. 052004. <https://doi.org/10.1063/1.4804672>
6. *Schnitzer O., Yariv E.* Nonlinear electrophoresis at arbitrary field strengths: small-Dukhin-number analysis // *Phys. Fluids*. 2014. Vol. 26. No. 12. P. 122002. <https://doi.org/10.1063/1.4902331>

7. *Tottori S., Misiunas K., Keyser U.F., Bonthuis D.J.* Nonlinear electrophoresis of highly charged nonpolarizable particles // *Phys. Rev. Lett.* 2019. Vol. 123. No 1. P. 014502. <https://doi.org/10.1103/physrevlett.123.014502>
8. *Khair A.S.* Nonlinear electrophoresis of colloidal particles // *Curr. Opin. Colloid Interface Sci.* 2022. Vol. 59. P. 101587. <https://doi.org/10.1016/j.cocis.2022.101587>
9. *Dukhin S.S.* Electrokinetic phenomena of the second kind and their applications // *Adv. Colloid Interface Sci.* 1991. Vol. 35. P. 173–196. [https://doi.org/10.1016/0001-8686\(91\)80022-c](https://doi.org/10.1016/0001-8686(91)80022-c)
10. *Yariv E.* Migration of ion-exchange particles driven by a uniform electric field // *J. Fluid Mech.* 2010. Vol. 655. Pp. 105–121. <https://doi.org/10.1017/s0022112010000716>
11. *Frants E.A., Ganchenko G.S., Shelistov V.S., Amiroudine S., Demekhin E.A.* Nonequilibrium electrophoresis of an ion-selective microgranule for weak and moderate external electric fields // *Phys. Fluids.* 2018. Vol. 30. No. 2. P. 022001. <https://doi.org/10.1063/1.5010084>
12. *Mishchuk N.A., Takhistov P.V.* Electroosmosis of the second kind // *Colloids Surf. A Physicochem. Eng. Asp.* 1995. Vol. 95. No. 2–3. Pp. 119–131. [https://doi.org/10.1016/0927-7757\(94\)02988-5](https://doi.org/10.1016/0927-7757(94)02988-5)
13. *Ganchenko G.S., Frants E.A., Shelistov V.S., Nikitin N.V., Amiroudine S., Demekhin E.A.* Extreme nonequilibrium electrophoresis of an ion-selective microgranule // *Phys. Rev. Fluid.* 2019. Vol. 4. No. 4. P. 043703. <https://doi.org/10.1103/physrevfluids.4.043703>
14. *Ganchenko G.S., Frants E.A., Amiroudine S., Demekhin E.A.* Instabilities, bifurcations, and transition to chaos in electrophoresis of charge-selective microparticle // *Phys. Fluids.* 2020. Vol. 32. No. 5. P. 054103. <https://doi.org/10.1063/1.5143312>
15. *Kłodzińska E., Szumski M., Dziubakiewicz E., Hrynkiewicz K., Skwarek E., Janusz W., Buszewski B.* Effect of zeta potential value on bacterial behavior during electrophoretic separation // *Electrophoresis.* 2010. Vol. 31. No. 9. Pp. 1590–1596. <https://doi.org/10.1002/elps.200900559>
16. *Polaczyk A.L., Amburgey J.E., Alansari A., Poler J.C., Propato M., Hill V.R.* Calculation and uncertainty of zeta potentials of microorganisms in a 1:1 electrolyte with a conductivity similar to surface water // *Colloids Surf. A Physicochem. Eng. Asp.* 2020. Vol. 586. P. 124097. <https://doi.org/10.1016/j.colsurfa.2019.124097>
17. *Maurya S.K., Gopmandal P.P., Ohshima H., Duval J.F.L.* Electrophoresis of composite soft particles with differentiated core and shell permeabilities to ions and fluid flow // *J. Colloid Interface Sci.* 2020. Vol. 558. Pp. 280–290. <https://doi.org/10.1016/j.jcis.2019.09.118>
18. *Ohshima H.* Approximate analytic expressions for the electrophoretic mobility of spherical soft particles // *Electrophoresis.* 2021. Vol. 42. No. 21–22. Pp. 2182–2188. <https://doi.org/10.1002/elps.202000339>
19. *Schnitzer O., Yariv E.* Streaming-potential phenomena in the thin-Debye-layer limit. Part 3. Shear-induced electroviscous repulsion // *J. Fluid Mech.* 2016. Vol. 786. Pp. 84–109. <https://doi.org/10.1017/jfm.2015.647>
20. *Frants E.A., Shelistov B.S., Ganchenko G.S., Gorbachev E.V., Alekseev M.S., Demekhin E.A.* Electrophoresis of a dielectric particle in a strong electric field // *Ekologicheskiy vestnik nauchnykh tsentrov Chernomorskogo ekonomicheskogo sotrudnichestva.* 2021. Vol. 18. No. 4. Pp. 33–40. <https://doi.org/10.31429/vestnik-18-4-33-40>
21. *Ganchenko G.S., Kalaidin E.N., Chakraborti S., Demekhin E.A.* Hydrodynamic instability under ohmic conditions in imperfect electrical membranes // *Doklady Akademii nauk.* 2017. Vol. 474. No. 3. Pp. 296–300. <https://doi.org/10.7868/s0869565217150063>
22. *Maduar S.R., Belyaev A.V., Lobaskin V., Vinogradova O.I.* Electrohydrodynamics near hydrophobic surfaces // *Phys. Rev. Lett.* 2015. Vol. 114. No. 11. P. 118301. <https://doi.org/10.1103/PhysRevLett.114.118301>
23. *Nikitin N.V.* Third-order-accurate semi-implicit Runge–Kutta scheme for incompressible Navier–Stokes equations // *Int. J. Numer. Methods Fluids.* 2006. Vol. 51. No. 2. Pp. 221–233. <https://doi.org/10.1002/fld.1122>
24. *Demekhin E.A., Nikitin N.V., Shelistov V.S.* Direct numerical simulation of electrokinetic instability and transition to chaotic motion // *Phys. Fluids.* 2013. Vol. 25. No. 12. P. 122001. <https://doi.org/10.1063/1.4843095>
25. *Shelistov V.S., Demekhin E.A., Ganchenko G.S.* Electrokinetic instability near charge-selective hydrophobic surfaces // *Phys. Rev. E.* 2014. Vol. 90. No. 1. P. 013001. <https://doi.org/10.1103/PhysRevE.90.013001>
26. *Ganchenko G.S., Shelistov V.S., Demekhin E.A.* Features of electrophoresis of a composite microparticle with a thin ion-selective shell // *Technical Physics Letters* (preparing for submission).